A Mutant in the *ADH1* Gene of *Chlamydomonas reinhardtii* Elicits Metabolic Restructuring during Anaerobiosis[1][W]

Leonardo Magneschi[2]*, Claudia Catalanotti, Venkataramanan Subramanian, Alexandra Dubini, Wenqiang Yang, Florence Mus, Matthew C. Posewitz, Michael Seibert, Pierdomenico Perata, and Arthur R. Grossman

Department of Plant Biology, Carnegie Institution for Science, Stanford, California 94305 (L.M., C.C., W.Y., A.R.G.); PlantLab, Institute of Life Sciences, Scuola Superiore Sant'Anna, Pisa 56124, Italy (L.M., P.P.); Biosciences Center, National Renewable Energy Laboratory, Golden, Colorado 80401 (V.S., A.D., M.S.); Colorado School of Mines, Department of Chemistry and Geochemistry, Golden, Colorado 80401 (V.S., M.C.P., M.S.); and Department of Microbiology, Department of Chemical and Biological Engineering, and Center for Biofilm Engineering, Montana State University, Bozeman, Montana 59717 (F.M.)

The green alga *Chlamydomonas reinhardtii* has numerous genes encoding enzymes that function in fermentative pathways. Among these, the bifunctional alcohol/acetaldehyde dehydrogenase (ADH1), highly homologous to the *Escherichia coli* AdhE enzyme, is proposed to be a key component of fermentative metabolism. To investigate the physiological role of ADH1 in dark anoxic metabolism, a *Chlamydomonas adh1* mutant was generated. We detected no ethanol synthesis in this mutant when it was placed under anoxia; the two other ADH homologs encoded on the *Chlamydomonas* genome do not appear to participate in ethanol production under our experimental conditions. Pyruvate formate lyase, acetate kinase, and hydrogenase protein levels were similar in wild-type cells and the *adh1* mutant, while the mutant had significantly more pyruvate:ferredoxin oxidoreductase. Furthermore, a marked change in metabolite levels (in addition to ethanol) synthesized by the mutant under anoxic conditions was observed; formate levels were reduced, acetate levels were elevated, and the production of CO_2 was significantly reduced, but fermentative H_2 production was unchanged relative to wild-type cells. Of particular interest is the finding that the mutant accumulates high levels of extracellular glycerol, which requires NADH as a substrate for its synthesis. Lactate production is also increased slightly in the mutant relative to the control strain. These findings demonstrate a restructuring of fermentative metabolism in the *adh1* mutant in a way that sustains the recycling (oxidation) of NADH and the survival of the mutant (similar to wild-type cell survival) during dark anoxic growth.

Photosynthetic microorganisms that have evolved in the soil, such as the unicellular green alga *Chlamydomonas reinhardtii* (*Chlamydomonas* throughout), are subjected to continuous fluctuations in oxygen availability and may experience anoxic or microaerobic conditions during the night and early morning, when low levels of photosynthesis combined with microbial respiration deplete the local environment of oxygen. The anoxic environment elicits the synthesis/activation of enzymes that ferment sugars, producing organic acids, ethanol, CO_2, and H_2 (Gfeller and Gibbs, 1984; Kreuzberg, 1984; Ohta et al., 1987). We and others are developing *Chlamydomonas* as a model system to elucidate pathways and regulatory circuits associated with fermentation metabolism in photosynthetic, eukaryotic microbes.

Chlamydomonas shares some metabolic features with both vascular plants and soil microbes. It relies on glycolytic breakdown of carbohydrate reserves and activation of fermentation pathways for generating the energy required for survival during periods of oxygen depletion (Gfeller and Gibbs, 1984; Kreuzberg, 1984; Ohta et al., 1987). A number of these fermentation pathways are typical of those present in various prokaryotes and some eukaryotes (Mus et al., 2007). Some

[1] This work was supported by the Office of Biological and Environmental Research, Genome to Life program, Office of Science, U.S. Department of Energy (grants to A.R.G., M.C. P., and M.S.), by the National Science Foundation (grant no. MCB–0235878) and the U.S. Department of Energy (grant no. DE–FG02–07ER64427) to A.R.G., by the Air Force Office of Scientific Research (grant no. FA9550–11–1–0211 to M.C.P.), by the Scuola Superiore Sant'Anna (to P.P. and L.M.), by the Regione Toscana (Programma Operativo Regionale Obiettivo 2 Fondo Sociale Europeo to L.M.), and by the National Renewable Energy Laboratory Pension Program (to M.S.). Work at the National Renewable Energy Laboratory was performed under U.S. Department of Energy contract number DE–AC36–08GO28308.

[2] Present address: Westfälische Wilhelms-Universität Münster, Institut für Biologie und Biotechnologie der Pflanzen, Hindenburgplatz 55, Munster 48143, Germany.

* Corresponding author; e-mail magneschi@sssup.it.

The author responsible for distribution of materials integral to the findings presented in this article in accordance with the policy described in the Instructions for Authors (www.plantphysiol.org) is: Leonardo Magneschi (magneschi@sssup.it).

[W] The online version of this article contains Web-only data.
www.plantphysiol.org/cgi/doi/10.1104/pp.111.191569

enzymes that function in these pathways include pyruvate:ferredoxin oxidoreductase (PFR), pyruvate decarboxylase (PDC), lactate dehydrogenase (LDH), pyruvate formate lyase (PFL), alcohol dehydrogenase (ADH), phosphate acetyltransferase (PAT), acetate kinase (ACK), and the two [FeFe] hydrogenases (HYDA1 and HYDA2) and their maturation proteins, HYDG and HYDEF (Posewitz et al., 2004; Atteia et al., 2006; Ghirardi et al., 2007; Mus et al., 2007; Hemschemeier et al., 2008; Grossman et al., 2011). The anaerobic activities of these and other enzymes result in the secretion of organic acids (formate, lactate, malate, acetate, and succinate) and alcohols (ethanol and glycerol) as well as the evolution of H_2 and CO_2 (Gfeller and Gibbs, 1984; Kreuzberg, 1984; Ohta et al., 1987; Tsygankov et al., 2002; Kosourov et al., 2003; Mus et al., 2007; Dubini et al., 2009).

When *Chlamydomonas* experiences dark anoxic conditions, the starch reserves, which are generated as a consequence of photosynthetic activity and stored in the chloroplast, are degraded to sugars, which may then be metabolized to pyruvate through glycolysis, leading to the production of ATP. Reduced pyridine nucleotides, cogenerated during this process, are reoxidized through the activities of several metabolic pathways that use glycolytic intermediates, primarily pyruvate, as the initial substrate (Fig. 1). Interactions among these pathways and the mechanisms by which they are regulated are still not completely understood.

Metabolites that are synthesized as cells ferment sugars, and the pathways responsible for their production in enteric bacteria have been known for many years (Harden, 1901; Clark, 1989).Fermentative metabolism in *Escherichia coli* and many other bacteria appears to have significant flexibility, and glycolytic NADH can be recycled during anaerobic metabolism by synthesizing and secreting various reduced metabolites, including ethanol, lactate, and succinate. Acetate is also generated as a consequence of fermentation, and while its synthesis from pyruvate generates ATP, it does not consume NADH. Recently, the flexibility associated with anaerobic metabolism in *Chlamydomonas* has been demonstrated through the generation and analyses of several mutant strains blocked for specific branches of

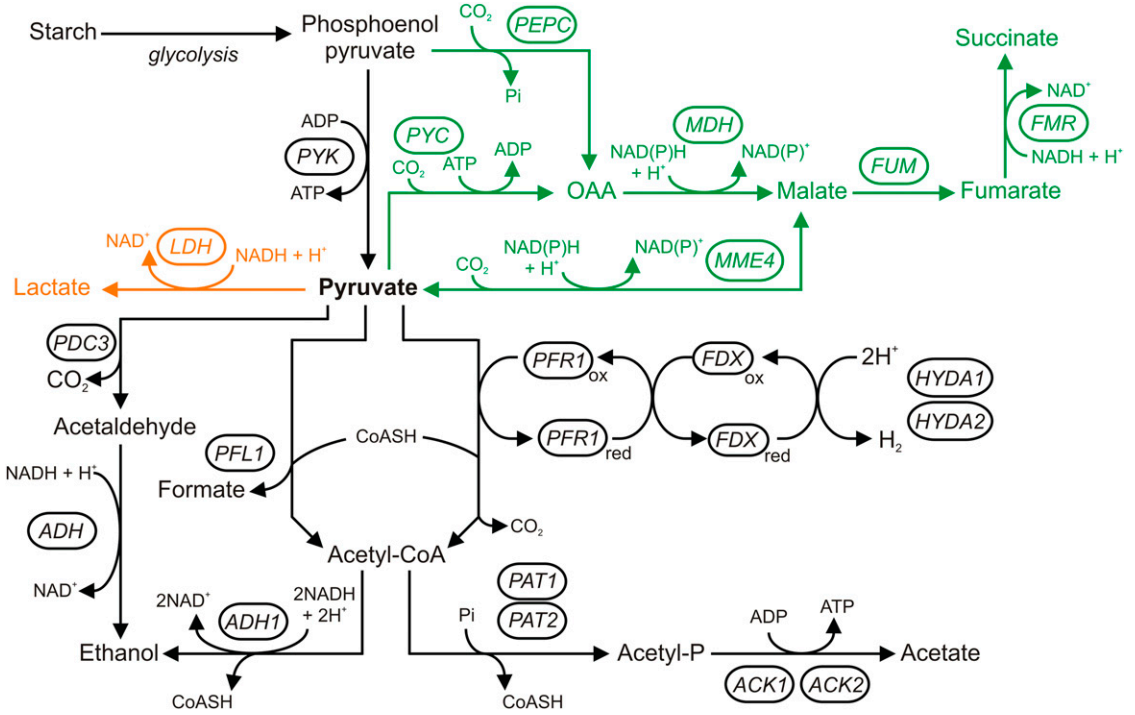

Figure 1. *Chlamydomonas* fermentative pathways under dark anoxic conditions. In wild-type cells (black arrows), the major fermentative products are formate, acetate, and ethanol, with CO_2 and H_2 emitted as minor products. The metabolic pathway that leads to the fermentative production of succinate is unveiled in the *hydEF-1* mutant (Dubini et al., 2009) and is depicted in the figure in green. An increase in the production of lactate, which is almost undetectable in fermenting wild-type cells, has been observed in the *pfl1* mutants (Philipps et al., 2011; Catalanotti et al., 2012) and is highlighted in orange. ACK1, Acetate kinase isoform 1; ACK2, acetate kinase isoform 2; ADH, alcohol dehydrogenase (ADH1, ADH2, or ADH3 could perform this reaction; see text); ADH1, acetaldehyde/alcohol dehydrogenase; FDX, ferredoxin; FMR, fumarate reductase; FUM, fumarase; HYDA1 and HYDA2, two putative hydrogenases; LDH, lactate dehydrogenase; MDH, malate dehydrogenase; MME4, malic enzyme; PAT1, phosphate acetyltransferase isoform 1; PAT2, phosphate acetyltransferase isoform 2; PDC3, pyruvate decarboxylase; PEPC, phosph*enol*pyruvate carboxylase; PFL1, pyruvate formate lyase; PFR1, pyruvate:ferredoxin oxidoreductase; PYC, pyruvate carboxylase; PYK, pyruvate kinase. This figure was modified from Grossman et al. (2011).

fermentation metabolism (Dubini et al., 2009; Grossman et al., 2011; Philipps et al., 2011; Catalanotti et al., 2012). For example, in the *Chlamydomonas hydEF-1* mutant (Dubini et al., 2009), pyruvate metabolism is redirected to the reverse tricarboxylic acid reactions, while in the *pfl1* mutant (Philipps et al., 2011; Catalanotti et al., 2012), there is a marked increase in lactate production and a smaller increase in ethanol synthesis; both of these metabolites are linked to NADH reoxidation (Fig. 1). The *pfl1* mutant cells also accumulate elevated intracellular levels of amino acids, which may help recycle NADH and limit the potentially damaging consequences of pyruvate accumulation (Gupta et al., 2009; Zabalza et al., 2009). Aspects of electron rerouting observed in the *Chlamydomonas pfl1* strain are similar to those observed for analogous *E. coli* mutants (Clark, 1989; Zhu and Shimizu, 2005), suggesting that the pathways and potentially some of the compensatory mechanisms are conserved between bacteria and eukaryotic green algae.

Under the fermentation conditions used, ethanol accounts for about one-fourth of the metabolites synthesized and excreted by *Chlamydomonas* cells during dark anoxia (Gfeller and Gibbs, 1984; Kreuzberg, 1984; Ohta et al., 1987). Cytoplasmic PDC and ADH activities typically ferment pyruvate to ethanol in terrestrial plants (Dolferus et al., 1985; Mücke et al., 1995; Kürsteiner et al., 2003; for review, see Magneschi and Perata, 2009). PDC catalyzes the decarboxylation of pyruvate to acetaldehyde and CO_2, while ADH reduces acetaldehyde to ethanol (Perata and Alpi, 1991; Perata et al., 1992), which is excreted from the organism. *Chlamydomonas* possesses three distinct enzymes that are potentially important for ethanol production when the cells become anoxic: ADH1 (a putative dual-function alcohol/acetaldehyde dehydrogenase, previously annotated as ADHE because of its homology with the *E. coli* AdhE protein [Mus et al., 2007; Hemschemeier et al., 2008]; Joint Genome Institute [JGI] version 4.0 protein identifier 133318, Augustus version 5.0 protein identifier 518335) and two other putative alcohol dehydrogenases that we designate ADH2 (JGI version 4.0 protein identifier 121409, Augustus version 5.0 protein identifier 516421) and ADH3 (JGI version 4.0 protein identifier 82021, Augustus version 5.0 protein identifier 516422). Analysis of protein sequences by InterProScan (http://www.ebi.ac.uk/Tools/pfa/iprscan/) suggests that both the alcohol and the aldehyde dehydrogenase domains are present in ADH2, whereas ADH3 possesses only the alcohol dehydrogenase domain. In the Enterobacteriaceae, the AdhE enzyme represents the major route for recycling NADH during fermentation (Clark and Cronan, 1980; Leonardo et al., 1996), as highlighted by the inability of an *E. coli adhE* mutant to grow on minimal medium under anoxic conditions (Cunningham and Clark, 1986; Gupta and Clark, 1989). Interestingly, an AdhE/ADH1 homolog is not present in the majority of prokaryotes, and among the eukaryotes, it has only been identified in a few amitochondriate protists and some green algae (Atteia et al., 2003, 2006). In the alga *Polytomella*, the ADHE protein was localized to the mitochondrion (Atteia et al., 2003), while in *Chlamydomonas*, ADH1 was found to be present in chloroplasts (Terashima et al., 2010). This difference in subcellular location, which could be explained by differences in targeting sequences located at the N terminus of the enzyme, may create differences in the intracellular trafficking of metabolites. Furthermore, the *Polytomella* ADHE protein lacks the conserved His residues in the ADH-IRON2 signature of the enzyme that are responsible for metal-catalyzed activation and oxygen sensitivity (Atteia et al., 2003; Supplemental Fig. S1). In contrast, *Chlamydomonas* ADH1 has retained the His-containing domain, which is also present in *E. coli* AdhE. These findings suggest that although *Chlamydomonas* ADH1 accumulates both at the transcript and protein levels under aerobic conditions (Whitney et al., 2011; this work), the protein might not be enzymatically active in an oxygen-containing atmosphere.

Based on sequence similarities with *E. coli* AdhE, the dual-function *Chlamydomonas* ADH1 protein has been suggested to operate downstream of PFL1, where it would reduce acetyl-CoA to acetaldehyde and then to ethanol, resulting in the regeneration of two molecules of NAD^+ per molecule of acetyl-CoA (Mus et al., 2007; Terashima et al., 2010; Grossman et al., 2011; Fig. 1). ADH1 transcript levels rise when *Chlamydomonas* cells are exposed to anoxic conditions (Mus et al., 2007; this work), and anaerobiosis caused a small increase in the level of the ADH1 protein (Terashima et al., 2010). The PDC (designated PDC3 in *Chlamydomonas*) pathway is also proposed to generate ethanol in *Chlamydomonas* (Fig. 1). Quantitative proteomics-based localization data have shown that the metabolism of pyruvate by the PFL1, PFR1, ADH1, and PAT2/ACK1 pathways occurs in *Chlamydomonas* chloroplasts, with parallel PFL1 and PAT1/ACK2 activities outside of the chloroplast, most likely in mitochondria (Terashima et al., 2010).

If ADH1 is responsible for ethanol production in the chloroplasts of *Chlamydomonas*, suppression of this activity could potentially lead to an increase in reducing equivalents in the chloroplast and elicit elevated hydrogenase activity, which would serve as an electron valve. In *E. coli*, *adhE* mutants exhibit increased acetate production and lower lactate/formate levels under microaerobic conditions, consistent with a down-regulation of both PFL and LDH activities in the mutant strain (Zhu and Shimizu, 2005). At this point, there is no experimental evidence that defines the participation of the three potential ADH proteins of *Chlamydomonas* in fermentative ethanol production. To address this issue, we exploited an insertional mutagenesis- and PCR-based reverse genetic screen (Pootakham et al., 2010; Gonzalez-Ballester et al., 2011) and identified a *Chlamydomonas adh1* mutant. Characterization of this mutant has allowed us to evaluate the impact of this enzyme on algal cells experiencing dark, anoxic conditions and to expand our understanding of the intricate relationships among the metabolic circuits

associated with pyruvate fermentation as well as the mechanisms associated with their control.

RESULTS

Identification of the *Chlamydomonas adh1* Mutant

To elucidate the function of ADH1 in *Chlamydomonas* metabolism, we generated an *adh1* insertional mutant. In this strain, the *aminoglycoside 3′-phosphotransferase* (*AphVIII*) marker gene is inserted into the 15th exon

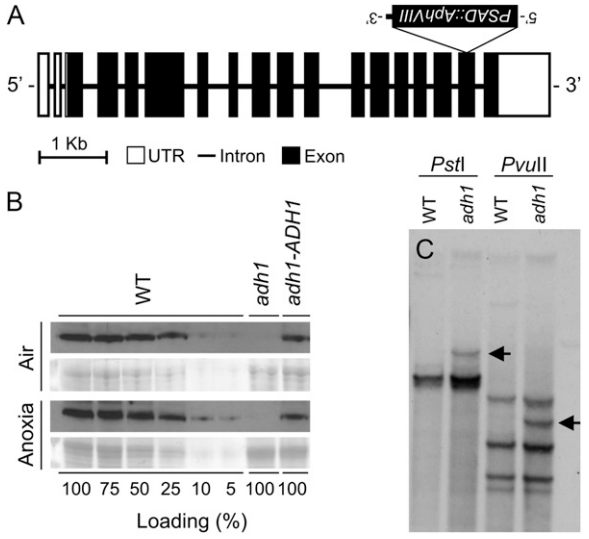

Figure 2. A *Chlamydomonas* mutant with an insertion in *ADH1*. A, Schematic representation of the insertion of the *AphVIII* cassette into *ADH1*. Note that the cassette is inserted in an inverted orientation relative to the *ADH1* gene. Insertion of the paromomycin cassette adds 18 amino acids to the ADH1 protein sequence before the occurrence of a translational stop codon; the final size of the protein is 954 amino acids in wild-type cells and 911 amino acids in the *adh1* mutant (893 amino acids from the wild-type ADH1 protein sequence and 18 amino acids from the noncoding strand of the paromomycin cassette). UTR, Untranslated region. B, The ADH1 protein cannot be detected in the mutant strain (*adh1* in the *CC-124* background) based on immunoblot analyses (with antibodies raised against the amino acid sequence SGTGSEVTPFSVVTD, which is upstream of the site of insertion) but is detected in wild-type *CC-124* cells (WT) and in the strain rescued by introduction of the *ADH1* coding sequence under the control of the PSAD promoter (*adh1-ADH1*). This promoter is able to drive expression of the reintroduced *ADH1* coding sequence under aerobic (Air) and anoxic (Anoxia; 4 h) conditions. Moreover, accumulation of the ADH1 protein in the rescued strain is stable over a 6-h anaerobic treatment (data not shown). The numbers below the panels indicate the relative amount of protein, with 100% corresponding to 45 μg of total protein loaded. C, Southern-blot analysis of genomic DNA from the original parental wild-type strain (*D66*) and the *adh1* mutant (in the original *D66* background) using the *AphVIII* cassette as a hybridization probe. The genomic DNA was digested with *Pst*I and *Pvu*II, as indicated. Arrows highlight the DNA band with the inserted *AphVIII* cassette; there appears to be only one copy of the cassette inserted into the *adh1* mutant genome.

of the coding region of *ADH1* (Fig. 2A) in an inverted orientation relative to the *ADH1* coding sequence. The insertion results in the synthesis of a mutated protein that is 43 amino acids shorter than the wild-type protein (911 compared with 954 amino acids), with the last 18 amino acids encoded by the fused marker gene sequence. Most of this aberrant polypeptide is likely rapidly degraded, as we were unable to detect the ADH1 protein by western-blot analyses of total proteins extracted from *adh1* mutant cells grown under either oxic or anoxic conditions (Fig. 2B). There is little change in the level of the *ADH1* transcript, based on reverse transcription and real-time quantitative (RT-q) PCR, in mutant relative to wild-type cells (see below), although the transcript would be aberrant in the mutant. The transformant analyzed here has a single copy of the *AphVIII* cassette integrated into its genome, as determined by Southern-blot hybridizations using the *AphVIII* cassette as the probe (Fig. 2C) as well as by segregation of the marker gene (always 1:1 segregation of paromomycin-resistant and -tolerant cells, with cosegregation of the resistant phenotype with the insertion in ADH1, suggesting the presence of a single marker gene insertion). The background bands on the Southern blot, which are the same in the wild-type (*D66*) and mutant strains, represent hybridizations to the *PSAD* promoter and to the *CYTc6* 3′ end, both of which are part of the *AphVIII* cassette.

A wild-type copy of the *ADH1* coding sequence under the control of the *PSAD* promoter was transformed into the *adh1* mutant. The transformant was rescued for ADH1 protein accumulation (Fig. 2B). Furthermore, for both the rescued *adh1* mutant and wild-type cells, the level of ADH1 protein was essentially the same during growth under aerobic and anoxic conditions (Fig. 2B).

Fitness of *adh1* following Exposure to Anoxic Conditions

We investigated the fitness of the *adh1* mutant to anoxic conditions. Reduction in plating efficiency for both mutant and wild-type cells was first noted 12 h after the shift to anoxic conditions, and by 18 h following this shift, most of the cells did not recover. Interestingly, the mutant shows a similar tolerance to anoxia as wild-type cells (Fig. 3). The similar behavior of mutant and wild-type cells suggests that the mutant may be able to compensate for the loss of ADH1 activity, possibly as a consequence of metabolic adjustments, although there might still be a difference in the fitness of these strains when they compete in their natural environment.

Transcript and Protein Abundances for Genes Encoding Fermentative Enzymes

To investigate how an inability to make ADH1 impacts the overall molecular responses of the cell to anoxia, we analyzed the levels of transcripts encoding key fermentative enzymes in mutant and wild-type

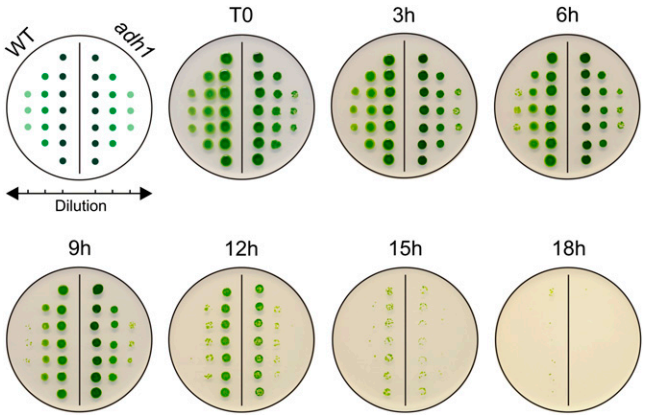

Figure 3. Anoxia tolerance of the wild type (WT) and the *adh1* mutant. The *adh1* and *CC-124* (wild-type) cells were grown under mixotrophic conditions in TAP medium until they reached midlog phase (around 2×10^6 cells mL^{-1}). Cells were then concentrated 10 times by centrifugation and resuspension in one-tenth of the initial volume of AIB buffer (Ghirardi et al., 1997). Culture concentrations were determined by counting the cells in aliquots of the culture using a hemocytometer; the cells, collected as five different aliquots from each sample, were counted and then averaged. For all samples, cell densities were equalized to 1.5×10^7 cells mL^{-1} (the final cultures were also counted three times to check for pipetting errors). Cultures were then subjected to dark anoxic treatment by purging the medium with argon for 30 min and incubating them for several hours inside an anaerobic workstation chamber. At specific time points (0, 3, 6, 9, 12, 15, and 18 h), 5 μL of culture was spotted onto the surface of TAP agar medium to allow viable cells to recover under aerobic conditions for 5 d to 1 week from the anoxic treatment. A light control (T0; cells spotted at 0 h of treatment and left under light aerobic conditions for 1 week) was also included to check for differences in the initial concentration of plated cells. As diagrammed in the top left petri dish with growing colonies, we performed two serial 1:10 dilutions of the treated cell cultures (with AIB) prior to plating them onto the solid medium; the left side of the petri dish always shows the growth of wild-type cells, while the right side always shows the growth of *adh1* mutant cells. Different spots within each column are technical replicates of the same dilution. Repetition of the experiment with two biological replicates yielded similar results.

cells. As shown in Figure 4, the levels of nearly all of the transcripts tested (except for PAT1 and PDC3) increased in wild-type cells exposed to anoxic conditions. In most cases, the mutant showed a similar response to that of wild-type cells. The level of *ADH1* mRNA in the *adh1* mutant (analyzed with primers designed upstream of the site of insertion) appeared to be approximately the same as in wild-type cells exposed to oxic or anoxic conditions, in spite of an interruption within the coding region of the gene. The levels of transcripts from *PFL1*, *PFR1*, *PDC3*, *HYDA1*, *HYDA2*, *PAT1*, *PAT2*, *ACK1*, and *ACK2* were either the same in wild-type and *adh1* mutant cells or, in some cases (*PAT2* and especially *PFR1*), significantly elevated in the *adh1* mutant relative to wild-type cells (Fig. 4).

The change in the level of a specific transcript did not always correlate with a change in the level of its encoded protein. The ADH1 protein was not detected in the *adh1* mutant under oxic or anoxic conditions by antibodies that recognize a sequence upstream of the site of insertion (Fig. 5), even though transcript abundance was high. This is not surprising, since it is not unusual for aberrant proteins, such as the truncated

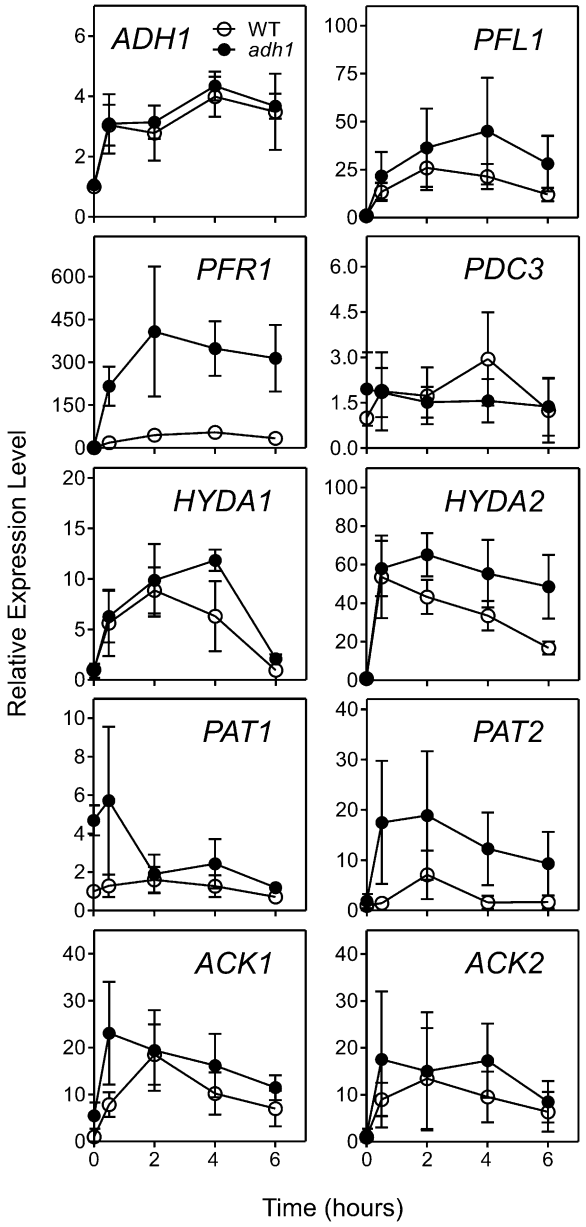

Figure 4. Levels of transcripts in wild-type (WT) and *adh1* mutant cells following exposure of cultures to anaerobic conditions (0, 0.5, 2, 4, and 6 h). The levels of transcripts encoding enzymes of the fermentative pathways were analyzed by RT-qPCR, using absolute quantification of the results that were normalized to transcript abundance at 0 h from *CC-124* (wild type [Steunou et al., 2006]; transcript levels at time 0 were arbitrarily made 1.0 for each of the tested transcripts). Data are means of two biological replicates, each with three technical replicates ± SD. The gene/protein names are as in Figure 1.

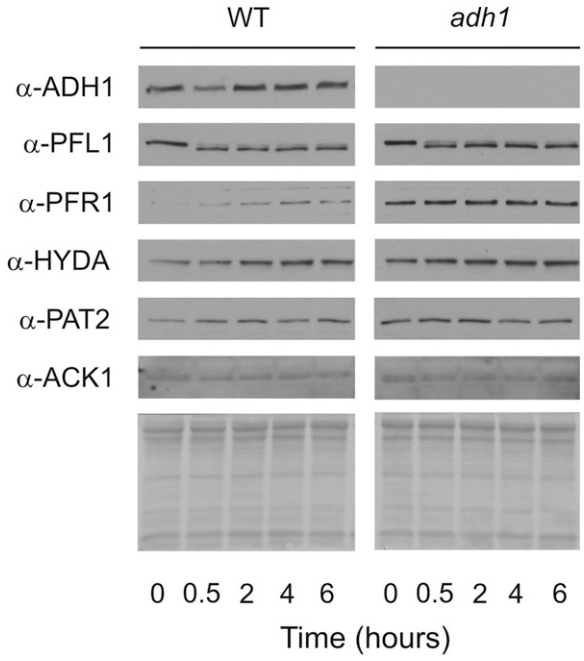

Figure 5. Western-blot analysis of fermentative enzymes in wild-type (WT) and *adh1* mutant cells. Amido black staining of the polyvinylidene difluoride membrane (bottom) is shown as a loading control. The time following the transfer of cells to anoxic conditions is given at the bottom. Note that the level of PFR1 is markedly up-regulated in the *adh1* mutant, while the levels of most other proteins are similar or slightly up-regulated (e.g. PAT2 and HYDA) in *adh1* relative to *CC-124* (wild-type) cells. The gene/protein names are as in Figure 1. Repetition of the experiment with two independent biological replicates yielded essentially identical results.

ADH1 protein of the mutant cells, to be rapidly degraded (Preiss et al., 2001). Western-blot analyses were not sensitive enough to detect the 1.5-fold increase in ADH1 protein after wild-type *Chlamydomonas* cells were transferred to anoxic conditions, which was reported previously (Terashima et al., 2010). However, while many transcripts, including those encoding *HYDA1*, *HYDA2*, *PFL1*, *ACK1*, and *PAT2*, increased significantly as the cells became anoxic, significant levels of the encoded proteins were already present in oxic cultures, and shifting to anoxic conditions caused little change in their abundances. However, it should be noted that the HYDA antibodies recognize both HYDA1 and HYDA2 and that the antibodies raised against PAT2 and ACK1 may also detect the PAT1 and ACK2 isoenzymes (Supplemental Fig. S2); although the predicted molecular sizes of the ACK proteins are different enough to be separated by SDS-PAGE (38 kD for ACK2 and 45 kD for ACK1), PAT isoforms have almost identical predicted masses, and even if the peptide sequence used to generate the PAT2 antibodies is highly modified in PAT1, the antibody might not be specific for PAT2. Furthermore, the mutant and wild-type cells exhibited similar levels of these proteins. Interestingly, the *PFR1* transcript accumulated to high levels in mutant cells, with a significantly lower level of accumulation in wild-type cells following a shift to anoxic conditions (Fig. 4). Also, while PFR1 protein levels in wild-type cells appear to be very low under oxic conditions and increased when the cells were exposed to anoxia, the *adh1* mutant had relatively high levels of PFR1 prior to exposing the cells to anoxic conditions, and the level remained high over the entire anoxic period (Fig. 5). These results demonstrated that *PFR1* transcript levels were not strictly coupled to protein production in the *adh1* mutant strain, suggesting that posttranscriptional processes (e.g. translation control, protein degradation) may have a strong impact, at least in some cases, on the final protein levels.

It has been suggested that the chloroplast-localized PAT2/ACK1 and ADH1 pathways compete for the substrate acetyl-CoA under conditions of oxygen deprivation (Mus et al., 2007; Terashima et al., 2010; Grossman et al., 2011). The PAT2/ACK1 pathway leads to the synthesis of acetate and ATP, while the ADH1 pathway would lead to the synthesis of ethanol, regenerating two NAD^+ (from two NADH) for each ethanol produced (Fig. 1). We examined the levels of the PAT and ACK proteins using antibodies generated to PAT2 and ACK1; however, as noted above, it is not clear that they are specific enough to distinguish between the two isoforms (chloroplast and likely mitochondrial) of these enzymes, especially between PAT2 and PAT1, which have nearly identical molecular masses (Supplemental Fig. S2). In our analyses, the PAT and ACK proteins accumulated to a similar extent in mutant and wild-type strains (Fig. 5). LDH and PDC3 are likely not present in chloroplasts (Terashima et al., 2010) and were not analyzed.

Extracellular Metabolite Production and H_2 Evolution

To directly evaluate the impact of the lack of ADH1 on changes in the activity of the various branches of fermentation metabolism, we analyzed the accumulation of metabolites excreted into the medium when wild-type and *adh1* cells transitioned from oxic to anoxic conditions. Ethanol production was completely abolished in the *adh1* strain (Fig. 6A), suggesting that the strain was indeed null for ADH1 activity, which is congruent with protein accumulation data. Furthermore, while PFR1 protein levels were shown to be significantly higher in the mutant than in wild-type cells (especially during the early stages of anoxia), the mutant showed little change in H_2 production under dark fermentative conditions (Fig. 6B). It is plausible that reduced ferredoxin generated by the PFR1 reaction could reduce substrates other than protons (e.g. sulfate, nitrite). The *adh1-ADH1* strain (wild-type copy of *ADH1* introduced into the mutant) is rescued for the production of ethanol (and other metabolites; Fig. 6) and makes somewhat more H_2 than wild-type cells (Fig. 6B). While acetate and formate levels increased in both the *adh1* mutant and wild-type cells following a shift to anoxic conditions (Fig. 6A), acetate accumu-

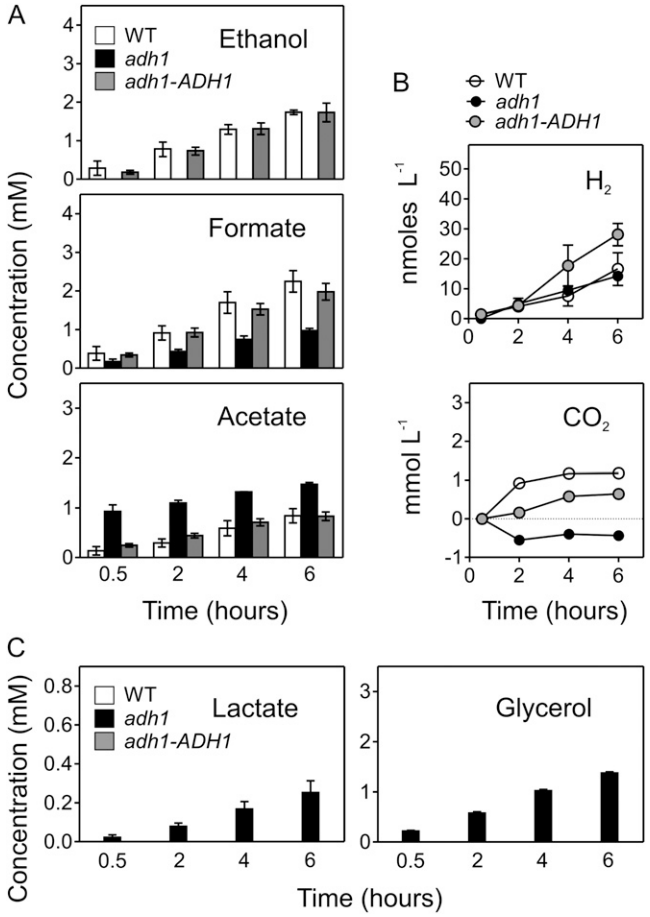

Figure 6. Metabolite levels in the wild type (WT), the *adh1* mutant, and the *adh1-ADH1* rescued strain under anoxic conditions. A, External levels of ethanol, formate, and acetate in *CC-124* (wild type), *adh1*, and *adh1-ADH1*. B, Fermentative H_2 production in the wild type, *adh1*, and *adh1-ADH1* (top) and fermentative CO_2 evolution in the wild type, *adh1*, and *adh1-ADH1* (bottom). The CO_2 data were calculated as the difference between the 30-min (anoxia) and time *x* (anoxia) values for the different *x* data points. C, Extracellular lactate accumulation in the wild type, *adh1*, and *adh1-ADH1* (left) and extracellular glycerol accumulation in the wild type, *adh1*, and *adh1-ADH1* (right). The data for all of the experiments presented in this figure were generated at 0.5, 2, 4, and 6 h following the imposition of anoxia and are expressed as means of three biological replicates ± SD. Note that wild-type cells and the rescued strain show neither lactate nor glycerol accumulation. In some instances, the error bars are so small that they are not seen (some external metabolite and CO_2 emission data).

lated to a significantly higher level in *adh1* than in wild-type cells, while the concentration of formate was much higher in wild-type cells following the shift to anoxic conditions (Fig. 6A). Furthermore, there was essentially no CO_2 production in the mutant strain (Fig. 6B). CO_2 production is most likely the consequence of PDC3 activity, which would generate acetaldehyde that would have to be reduced to ethanol by ADH or, potentially, from the PFR1 reaction if protons (through hydrogenase) are not the ultimate electron acceptor. The inability of the *adh1* mutant to accumulate ethanol and CO_2, with low levels of formate production, suggests that the acetaldehyde produced by PDC3 and the acetyl-CoA produced by PFL1 and PFR1 are not readily reduced in mutant cells exposed to anoxic conditions and that under such conditions the activities of PFL1 and PDC3, the major producers of formate and CO_2, respectively, may decline. These findings also strongly suggest that ADH1 is the only putative alcohol dehydrogenase in *Chlamydomonas* cells that is capable of reducing acetyl-CoA or acetaldehyde under the conditions used in this study.

Changes in fermentative metabolism in *adh1* cells would be critical to limit the generation and buildup of substrates normally acted on by ADH1, allowing the mutant to accommodate the block in ethanol production. However, it would also be necessary for the mutant to eliminate reducing equivalents that are generated during the glycolytic production of ATP. The *adh1* strain did show some extracellular lactate accumulation, which was not observed in wild-type cells (Fig. 6C); however, a significantly larger increase in lactate accumulation was observed in strains lacking PFL1 (Philipps et al., 2011; Catalanotti et al., 2012). Furthermore, transcript levels for LDH were identical in *adh1* and wild-type cells over the entire anoxic time course (Fig. 7). Most interesting was the finding that the medium of the *adh1* mutant contained high levels of glycerol relative to wild-type cells when the cultures became anoxic (Fig. 6C); internal metabolite analysis also showed higher intracellular glycerol levels in *adh1* relative to the wild-type cells (Supplemental Table S2). Extracellular lactate and glycerol do not accumulate in the rescued strain (Fig. 6C). Glycerol is synthesized from dihydroxyacetone phosphate (DHAP). This metabolite precedes the formation of pyruvate and the 3C oxidation (NADH formation) step in glycolysis, and glycerol synthesis also effectively recycles one NADH. Hence, the production of glycerol and lactate in the *adh1* mutant, as highlighted in the diagram of fermentation metabolism presented in Figure 8, would allow for the efficient recycling of NADH, an activity critical for maintaining redox balance and sustaining glycolytic production of ATP, even though the cells are unable to reduce acetaldehyde or acetyl-CoA to ethanol.

The conversion of DHAP into *sn*-glycerol-3-phosphate, a metabolic intermediate in glycerol synthesis, occurs through the activity of the enzyme *sn*-glycerol-3-phosphate dehydrogenase (GPD); *sn*-glycerol-3-phosphate synthesis and GPD activities were shown to be present in isolated *Chlamydomonas* chloroplasts during plastidic starch degradation in the dark (Klöck and Kreuzberg, 1989). The *Chlamydomonas* genome contains five genes encoding putative GPD enzymes; we named these genes *GPD1* (Augustus version 5.0 identifier 513084), *GPD2* (Augustus version 5.0 identifier 511717), *GPD3* (Augustus version 5.0 identifier 511720), *GPD4* (Augustus version 5.0 identifier 509652), and *GPD5* (Augustus version 5.0 identifier 343023). We also investigated whether the observed accumulation of glycerol in *adh1* mutant

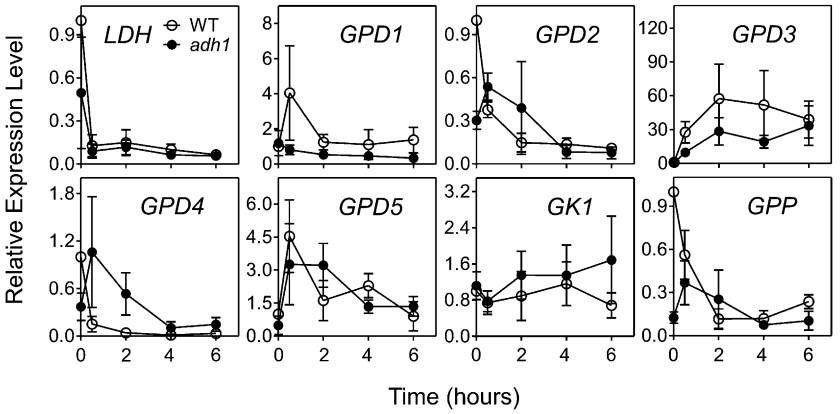

Figure 7. Levels of transcripts encoding LDH, GPD (*GPD1*, *GPD2*, *GPD3*, *GPD4*, and *GPD5*), *GK1*, and *GPP* in *CC-124* (wild-type [WT]) and *adh1* cells following exposure of cultures to anaerobic conditions (0, 0.5, 2, 4, and 6 h). The levels of transcripts were analyzed by RT-qPCR using absolute quantification of results that were normalized to transcript abundance at 0 h from the wild type, as performed previously (Steunou et al., 2006). Data are means of two biological replicates each with three technical replicates ± SD.

cells was linked to increased levels of transcripts encoding the GPDs (Fig. 7). While there was substantial variability in the data, we observe that the levels of some of *GPD* transcripts increased in wild-type and mutant cells following the transition from oxic to anoxic conditions (*GPD3* and *GPD5*). Also, there do appear to be slightly higher levels of the *GPD4* transcript in the mutant relative to wild-type cells (although in both, the transcript levels decline). More work is required to determine if the level of GPD activity changes as the cells become anoxic and the roles of the different isozymes in glycerol production. The subsequent conversion of *sn*-glycerol-3-phosphate to glycerol requires either the enzyme glycerol kinase (GK) or glycerol 3-phosphate phosphatase (GPP), both encoded by single genes in the *Chlamydomonas* genome. Transcript abundances for both *GK1* (Augustus version 5.0 identifier 522152) and *GPP* (Augustus version 5.0 identifier 519809) are comparable in *adh1* and wild-type cells experiencing anoxia (Fig. 7).

DISCUSSION

To elucidate the physiological role of *Chlamydomonas* ADH1, the *E. coli* AdhE homolog, we generated and characterized an *adh1* insertional mutant. Analysis of this mutant suggests that ADH1 in this unicellular alga catalyzes the dominant activity that reoxidizes NADH under anoxic conditions, a key reaction that allows glycolysis to continue to operate and to generate the energy needed for survival when cells lack oxygen as a terminal electron acceptor. The *adh1* mutant cannot synthesize ethanol (below the detection limit under the conditions that we are using), which

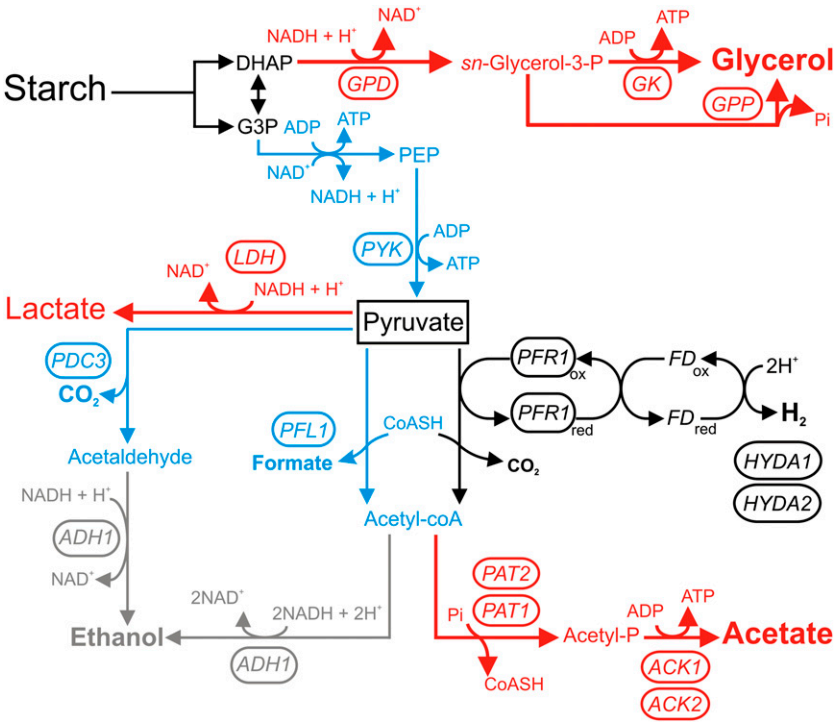

Figure 8. Pathways responsible for metabolite accumulation in wild-type and *adh1* mutant cells. Red arrows indicate pathways that appear to be up-regulated, and blue arrows indicate pathways that appear to be down-regulated, in the *adh1* mutant relative to wild-type cells. Black arrows indicate reactions that do not appear to be significantly altered in mutant relative to wild-type cells. Gray arrows show pathways for which a product was not detected in *adh1* mutant cultures but is normally detected in wild-type cultures. This schematic is based on metabolite abundances only. The gene/protein names are as in Figure 1. This figure was modified from Grossman et al. (2011).

strongly suggests that most ethanol produced during anoxia is a consequence of ADH1 activity and that the other potential ADH proteins in *Chlamydomonas* cannot compensate for this loss (either because they are not able to reduce acetaldehyde and acetyl-CoA or because of their different subcellular localizations or expression patterns). Indeed, protein sequence analysis reveals that the domain required for aldehyde dehydrogenase activity is missing in ADH3 and that there are modifications in ADH2 of conserved sequences associated with the first putative nucleotide-binding domain and the catalytic center of the protein (Supplemental Fig. S1). This catalytic center is conserved in all CoA-dependent and CoA-independent aldehyde dehydrogenases (Atteia et al., 2003). Our results also strongly suggest a critical coupling of the output of the PDC3 and PFL1 reactions (acetaldehyde and acetyl-CoA, respectively) in *Chlamydomonas* with ADH1 activity. A similar coupling between PFL and AdhE in *E. coli* has been reported (for review, see Clark, 1989). Although other pathways in *Chlamydomonas* may generate acetaldehyde or acetyl-CoA (substrates for ADH1 and ethanol production), elevated CO_2 evolution in sodium hypophosphite-treated cultures (in which PFL activity is irreversibly blocked; Knappe et al., 1984; Plaga et al., 1988) implicates PDC3/ADH coupled reactions in the production of ethanol (Hemschemeier et al., 2008; Catalanotti et al., 2012). ADH1 and/or one of the other two putative ADH proteins in *Chlamydomonas* could potentially work in conjunction with PDC3 (previously referred to as PDC1 and PDC by Mus et al. [2007] and Terashima et al. [2010], respectively) to help manage intracellular redox conditions during anaerobiosis, especially when PFL1 activity is reduced or impaired. However, the work presented here suggests that it is predominantly ADH1 that catalyzes the reduction of the acetaldehyde generated by PDC3 (Catalanotti et al., 2012; this paper), at least under the conditions used in our experiments. This coupling raises some issues concerning the way in which ADH1 accesses acetaldehyde, since the ADH1 protein was found exclusively in chloroplasts of *Chlamydomonas*, while PDC3 (which has no apparent transit peptide) was putatively cytoplasmic; acetaldehyde would have to traffic into plastids to be reduced to ethanol. The function(s) of the other putative ADH activities in wild-type *Chlamydomonas* cells is not clear, although they may have significant roles in fermentation and ethanol synthesis under specific environmental conditions, or they may represent NADH aldehyde dehydrogenases with unique specificities.

It is noteworthy that *E. coli* mutants defective for AdhE do not grow anaerobically on Glc, even though the strains do have LDH activity. This growth defect may reflect the fact that any acetyl-CoA that is generated by PFL in *adhE* mutants can only be metabolized through the PAT/ACK pathway. While this would lead to the production of an extra 1 mol ATP mol^{-1} Glc, it would not allow for oxidative recycling of NADH, which is critical for sustaining glycolysis and ATP production. Similarly, vascular plants that lack ADH activity are also more sensitive to anoxic conditions (Jacobs et al., 1988; Saika et al., 2006). These results demonstrate the critical nature of ADH activity in maintaining energy/redox balance and sustained viability when organisms are exposed to anoxic conditions.

Our results show that *Chlamydomonas* is able to adjust to the lack of the ADH1 protein, thus surviving equally well as wild-type cells under anoxic conditions (Fig. 3); the anoxic tolerance of the *adh1* mutant might reflect specific compensatory metabolic changes. Indeed, in addition to eliminating the production of ethanol, the *ADH1* gene disruption elicits marked alterations in the levels of a number of secreted metabolites, including acetate, formate, lactate, and glycerol. Previous work has shown that blocking various reactions associated with fermentation metabolism can cause changes in the flow of metabolites through other branches of the fermentative network. For example, *Chlamydomonas* strains lacking PFL1 (Philipps et al., 2011; Catalanotti et al., 2012) compensate for the loss of this activity by increasing the synthesis of lactate through the activity of LDH, an enzyme that in wild-type cells would compete with PFL1 for the substrate pyruvate. Hence, a proportion of the pyruvate that accumulates in the *pfl1* mutant would be metabolized by LDH, resulting in the accumulation of lactate and the reoxidation of 1 mol of NADH, which would help sustain the catabolism of polysaccharides and the synthesis of ATP in the mutant (Fig. 1). Similarly, an *E. coli pfl* mutant can grow anaerobically on acetate by maintaining energy production by metabolizing pyruvate to lactate (Clark, 1989). Indeed, the LDH enzyme of *E. coli* has been reported to be allosterically regulated, with elevated activity associated with increased pyruvate concentrations (Tarmy and Kaplan, 1968), suggesting that this enzyme has an overspill function (Clark, 1989). Another example of the metabolic flexibility of *Chlamydomonas* and alternative strategies to sustain ATP production when a specific branch of anaerobic metabolism is blocked comes from studies of the *hydEF-1* mutant (Dubini et al., 2009). This mutant can no longer eliminate reducing equivalents through H_2 synthesis, although it appears to sustain anaerobic ATP production by the activation of reverse tricarboxylic acid reactions. These reactions consume reducing equivalents and generate succinate, which can be exported from the cell (Fig. 1).

Analogous to the consequences of metabolic blocks that have been reported in previous studies (Dubini et al., 2009; Philipps et al., 2011; Catalanotti et al., 2012), a block in the conversion of acetaldehyde and acetyl-CoA to ethanol leads to the rerouting of metabolites to other pathways in the fermentation network; some of these pathways are marginally active in wild-type cells. For the *adh1* mutant placed under anoxic conditions, the level of extracellular formate is decreased while the level of acetate is increased relative to wild-

type cells. This suggests a reduction in PFL1 activity and a greater flux of acetyl-CoA through the PAT2/ACK1 pathway, which is NADH neutral. Fermentative H_2 production is not altered in *adh1* cells, in spite of the increases observed in *PFR1* transcript and protein levels. These results suggest that limitations in the production of H_2 are not at the level of PFR1 and/or that other regulatory/metabolic features of the system limit the flow of electrons to the hydrogenase in the *adh1* mutant.

A major rerouting of metabolism in the *adh1* mutant is reflected by the accumulation of the extracellular metabolites lactate and glycerol, which are not detected in cultures of anoxic wild-type cells (Fig. 6C). On the other hand, CO_2 evolution is decreased (Fig. 6B), which likely reflects metabolite redirection away from PDC3, regardless of the level of PDC3 in the cells. The evolutionary logic in this metabolic rewiring requires careful consideration of the functioning of glycolysis under anoxic conditions and the consequences of eliminating a major reaction critical for the recycling of reduced pyridine nucleotide. Glycolytic reactions convert Glc to two molecules of pyruvate, and in the process, it produces two NADH molecules that must be reoxidized to sustain continued glycolytic ATP formation (which is needed to maintain cell viability). The fermentation profile observed in the *adh1* mutant indicates that approximately half of the glycolytic flux in the mutant is being converted to glycerol and half to pyruvate (with the pyruvate converted mostly to formate/acetate and lactate). Glycerol is metabolically derived from DHAP, a 3C glycolytic intermediate that precedes NADH production in glycolysis. Additionally, one NADH is oxidized by GPD in the conversion of DHAP to *sn*-glycerol-3-phosphate, an intermediate in the formation of glycerol. In summary, in the glycolytic breakdown of a 6C sugar in the *adh1* mutant, the diversion of approximately one DHAP (3C) to glycerol synthesis eliminates the production of an NADH, and the NADH that is formed in the conversion of the other DHAP to pyruvate would be oxidized in the synthesis of glycerol, resulting in a near net zero production of reduced pyridine nucleotide (Fig. 8), although some NADH would also be recycled through the LDH reaction. This rerouting of carbon flow would dramatically reduce the need for the cells to reoxidize NADH (they would not generate as much), which would allow much of the acetyl-CoA synthesized during the fermentative breakdown of pyruvate to be metabolized to acetate in a reaction that does not require reductant but that does synthesize an ATP in addition to those generated by glycolysis. This change in metabolic flux is reflected by the appearance of glycerol (Fig. 6C) and increased acetate accumulation (Fig. 6A) in the medium of the *adh1* mutant relative to wild-type cells.

An increase in the levels of some *GPD* transcripts (*GDP3* and *GDP5*) does occur in both wild-type cells and the *adh1* mutant as the cells transition from aerobic to anoxic conditions (Fig. 7). Whether these increases in transcript levels are necessary for the synthesis of the extracellular glycerol that accumulates in the mutant strain has yet to be established (they are clearly not sufficient for the increased glycerol production, since they occur in both wild-type and mutant cells). In the green halotolerant alga *Dunaliella tertiolecta*, it was shown that neither de novo protein synthesis nor covalent modification of GPD is involved in glycerol production in response to hyperosmotic shock (Belmans and van Laere, 1987; Sadka et al., 1989).

To our knowledge, this work represents the first evidence for glycerol accumulation in *Chlamydomonas* under anaerobic conditions when alternative NADH-oxidizing pathways are disrupted. In order to more thoroughly understand the fermentation circuits and their regulation in *Chlamydomonas*, it is important to generate additional mutants (single, double, and triple mutants) to characterize how specific lesions alter both internal and external metabolite pools, to define the catalytic features of the various enzymes associated with fermentation metabolism and their potential interactions with each other, and to understand how redox and metabolite levels modulate the activities of the various fermentative pathways. It is also critical to define the different compartments that house the glycolytic reactions, pyruvate metabolism, and the fate of the various pyruvate breakdown products. Interestingly, the significant similarity of *Chlamydomonas* fermentation to various aspects of fermentation in the Enterobacteriaceae, such as *E. coli*, raises the question of when and how these metabolic pathways were acquired by green algae. Recently, it was suggested that a horizontal gene transfer that occurred after the divergence of the primary endosymbiotic algal lineages is likely responsible for the presence of eubacteria-type Gln synthethase II in Chloroplastida such as *Chlamydomonas* (Ghoshroy et al., 2010). Therefore, some genes encoding enzymes for key metabolic reactions in the green algal lineage, and that function within chloroplasts, may have originated as a consequence of a lateral gene transfer. In some cases, the transferred genes are likely to have come from γ-proteobacteria (Ghoshroy et al., 2010). *Chlamydomonas* chloroplasts were reported to possess all the enzymes necessary for the conversion of Glc-6-P to CO_2 and water under dark conditions (Chen and Gibbs, 1991). The initial reactions of glycolysis (Glc-6-P to glyceraldehyde-3-phosphate) and the oxidative pentose phosphate pathway are present in *Chlamydomonas* chloroplasts (Klein, 1986). However, it is still unclear whether complete glycolytic breakdown of Glc to pyruvate occurs in chloroplasts of anaerobic *Chlamydomonas* cells. It is also unclear how much NADH recycling occurs in chloroplasts of anaerobic cells. However, based on our results, most regeneration of NAD^+ from NADH in anaerobic wild-type *Chlamydomonas* cells requires chloroplast ADH1 activity. Furthermore, essentially all of the work reported by us and others suggests that there is regulated integration of fermentation pathways in *Chlamydomonas*, which is

probably also the case for other soil-dwelling algae. The analysis of the *adh1* mutant represents another example of the extraordinary ability of *Chlamydomonas* to modulate the activities of the various fermentative pathways in order to maintain redox balance and the production of ATP during anoxia, thus surviving the anaerobic stress. The precise mechanisms used to achieve physiological integration are still to be elucidated.

MATERIALS AND METHODS

Strains and Growth Conditions

Chlamydomonas reinhardtii wild-type strains *CC-124* (*nit*$^{2-}$, *mt*$^{-}$) and *D66* (CC-4425, *nit*$^{2-}$, *cw15*, *mt*$^{+}$; Schnell and Lefebvre, 1993; Pollock et al., 2003) and the *adh1* mutant in both the *CC-124* and *D66* genetic backgrounds were maintained on Tris-acetate-phosphate (TAP) medium, pH 7.2, solidified with 1.2% (w/v) agar at 25°C and 80 μmol photon m^{-2} s^{-1} photosynthetically active, constant irradiance. A PCR-amplified DNA cassette (1.7 kb) encoding a protein that confers paromomycin resistance (*AphVIII*) was used to transform *Chlamydomonas* cells, generating a library of *Chlamydomonas* insertional mutants (Pootakham et al., 2010; Gonzalez-Ballester et al., 2011). The *adh1* mutant allele was isolated from this library (*D66* genetic background) using a PCR-based screen (Pootakham et al., 2010; Gonzalez-Ballester et al., 2011) with the *ADH1*-specific primers listed in Supplemental Table S1. The mutant was backcrossed four times with *CC-124*. The *CC-124* and *adh1* strains (*CC-124* genetic background) were grown on solid TAP medium, and once the cells were near confluence on the plate, they were transferred to liquid TAP medium (approximately 50 mL) and grown for 1 d at 25°C, 80 μmol photon m^{-2} s^{-1} photosynthetically active, constant irradiance. These liquid cultures were used to inoculate 900 mL of TAP medium, pH 7.2, to a final concentration of 5×10^4 cells mL^{-1} (cells were counted three times for accuracy using a hemocytometer). TAP cultures were grown in Roux bottles, stirred using a magnetic stir bar, and vigorously bubbled with air enriched with 3% CO_2. Typically, experiments were performed with cultures that were grown subsequently for 2 d to a final density of approximately 2×10^6 cells mL^{-1}.

Anaerobic Induction, Sampling, and Survival

Chlamydomonas cultures grown on liquid TAP medium (approximately 2×10^6 cells mL^{-1}) were concentrated 10 times by centrifugation (2,500*g* for 1 min) and subsequent resuspension in 0.1 volume of anaerobic induction buffer (AIB) containing 50 mM potassium phosphate (pH 7.0) and 3 mM $MgCl_2$ (Ghirardi et al., 1997). The AIB suspended cultures were at 2×10^7 cells mL^{-1} (1.5×10^7 cells mL^{-1} for tolerance assays). These cultures were flushed with argon for 30 min and then incubated under anaerobic conditions (inside an anaerobic chamber; Coy Laboratory Products) at room temperature in the dark. Cells were collected at 4°C by centrifugation (10,000*g* for 1 min) at specific times after the imposition of anoxia, and the supernatants and pellets were separated, frozen in liquid nitrogen, and stored at −80°C for later analyses (e.g. protein and nucleic acid). As an estimation of cell viability following the anoxic treatment, aliquots of the cultures were sampled every 3 h over an 18-h period and spotted as serial 1:10 dilutions onto the surface of solid TAP medium to allow for the recovery of viable cells. Each spot represented 5 μL of a culture at an initial density of 1.5×10^7 cells mL^{-1} (or 1:10 and 1:100 dilutions; see the columns on each plate in Fig. 3). A control sample maintained under aerobic conditions in the light was included in the survival tests.

Southern-Blot Analyses

Genomic DNA was isolated from 50-mL liquid cultures of *Chlamydomonas D66* and the original *adh1* mutant (*D66* background), each at 2×10^6 cells mL^{-1}, using a standard phenol-chloroform extraction protocol (Sambrook et al., 1989). Ten micrograms of genomic DNA was digested for 2 h with 10 units of *Pst*I or *Pvu*II restriction endonucleases (New England Biolabs), the DNA fragments were separated by agarose (0.8%) gel electrophoresis, the gels were blotted overnight in 20× SSC onto nylon membranes (Bio-Rad), and the transferred DNA was cross-linked to the membrane by UV illumination. An alkaline phosphatase-labeled DNA probe was synthesized by chemically cross-linking a thermostable alkaline phosphatase to the 1.7-kb *AphVIII* PCR fragment (Sizova et al., 2001), which also contains the *PSAD* promoter and the 3′ sequence from the *CYTc6* gene (Fischer and Rochaix, 2001). Probe synthesis and hybridizations were performed using the Amersham AlkPhos Direct Labeling and Detection System according to the manufacturer's protocol (Amersham Biosciences). Cross-linked, membrane-bound, genomic DNA was hybridized overnight with the alkaline phosphatase-linked, 1.7-kb *AphVIII* PCR product.

Extraction of RNA

Total RNA was isolated from frozen cell pellets using a standard phenol-chloroform extraction protocol (Sambrook et al., 1989). The RNA was precipitated overnight in 4 M LiCl (final concentration) at 4°C to eliminate most of the DNA in the preparations. To completely free the sample of genomic DNA, approximately 40 μg of the RNA was treated with 5 units of RNase-free DNase I (Qiagen) for 1 h at room temperature (and repeated if necessary). A Qiagen RNeasy MinElute kit was used to purify the DNase-treated total RNA and remove degraded DNA, tRNA, 5.5S rRNA, DNase, contaminating proteins, and potential inhibitors of the RT reaction. The A_{260} of the eluted RNA was determined, and its integrity was evaluated by electrophoresis on formaldehyde agarose gels.

RT-qPCR

The abundance of specific transcripts in the total mRNA of each sample was quantified by RT-qPCR using the Engine Opticon system (Bio-Rad). First-strand cDNA synthesis was primed from purified, total RNA template using specific primers for each *Chlamydomonas* transcript that was examined. The RT reaction conditions were reported previously (Mus et al., 2007; Dubini et al., 2009); forward and reverse primer sequences used in the RT-qPCR are listed in Supplemental Table S1. Amplifications were performed using the following specific cycling parameters: an initial, single step at 95°C for 10 min (denaturation), then 40 cycles of 95°C for 30 s (denaturation), 60°C for 45 s (annealing), and 72°C for 30 s (elongation), and then fluorescence measurement after holding the reaction at 80°C for 10 s. This last step was incorporated into the protocol to avoid background signals resulting from primer dimer formation. After completing the 40 cycles, a final elongation step was performed at 72°C for 10 min. Melt curves (65°C–100°C, heating rate of 0.2°C s^{-1} with continuous fluorescence measurements) were evaluated for all PCRs to ensure that single DNA species were amplified. We determined both the absolute (Steunou et al., 2006) and relative levels of each specific RNA (normalized to the T0 sample corresponding to oxic conditions). All reactions were performed in triplicate with at least two biological replicates.

Protein Isolation, SDS-PAGE, and Immunoblot Analysis

Frozen cell pellets were thawed and resuspended in 50 mM Tris buffer (pH 8.0) containing 10 mM EDTA, 2% SDS, 1 mM phenylmethylsulfonyl fluoride, and 1 mM benzamidine-HCl. Protein concentrations were determined by the bicinchoninic acid assay (Thermo Fisher Scientific) as described by the manufacturer. For PAGE of proteins, pelleted cells were resuspended in 2% SDS and 1 mM β-mercaptoethanol and then boiled for 5 min. Solubilized proteins were separated by SDS-PAGE on a 10% polyacrylamide gel and then transferred to polyvinylidene difluoride membranes by a Bio-Rad Trans-Blot SD Semi-Dry Electrophoretic Transfer Cell following the manufacturer's instructions. The membranes were blocked in a 5% suspension of powdered milk in Tris-buffered saline (pH 8.0) with 0.1% Tween 20 for 1 h prior to an overnight incubation in the presence of primary antibodies. Dilutions of the primary antibodies used were as follows: 1:20,000 for α-PFL1, 1:5,000 for α-HYDA, 1:1,000 for α-PFR1, 1:2,000 for α-PAT2, 1:500 for ACK1, and 1:1,000 for ADH1. A 1:10,000 dilution of horseradish peroxidase-conjugated anti-rabbit IgG (Promega) was used as a secondary antibody. The peroxidase activity was detected by an enhanced chemiluminescence assay (GE Healthcare).

Antibodies

Antibodies were prepared by Agrisera (http://www.agrisera.com/en/info/home.html) against the synthesized peptides EWLSHENRFQILERK,

RSGRNYARDTIDRIF, and SGTGSEVTPFSVVTD of the *Chlamydomonas* PFR1, PAT2, and ADH1 proteins, respectively. These peptides were conjugated to keyhole limpet hemocyanin carrier protein via a Cys that was added to the N terminus of each peptide. ACK1 antibodies were generated against the full-length recombinant protein. PAT and ACK antibodies might recognize the two isoforms (chloroplast and likely mitochondrial) of these enzymes (Supplemental Fig. S2). Hydrogenase levels were evaluated by commercial antibodies that recognize both HYDA1 and HYDA2 (Agrisera; no. AS09 514). PFL1 antibodies were kindly provided by Ariane Atteia at the Laboratoire de Bioénergétique et Ingénierie des Protéines in Marseille, France.

Extracellular Metabolite Analysis

Organic acids and alcohols were analyzed by liquid chromatography using a Hewlett-Packard Series 1200 HPLC device. Dark-adapted cells were collected at various times following the imposition of anoxic conditions and pelleted by a 1-min centrifugation (10,000*g*), and the supernatant was transferred to a new vial and frozen in liquid N_2 for subsequent analysis. For organic acid analyses, the samples were thawed, centrifuged, and filtered prior to the injection of 100 μL of the supernatant onto an Aminex HPX-87H (300 $\times$ 7.8 mm) ion-exchange column. Metabolites in the supernatant were separated on the column using filtered 8 mM sulfuric acid as the mobile phase; the flow rate was 0.6 mL min^{-1} at 45°C. Organic acid retention peaks were recorded using Agilent ChemStation software and quantified by comparisons with absorption of known amounts of a standard for each of the organic acids. Ethanol was detected using the refractive index detector attached to the HPLC apparatus.

CO_2 and H_2 Measurement

CO_2 levels were below detection limits in the serum vial head space of anaerobically acclimated cells. Therefore, following anaerobic induction, 1 mL of anoxic cells was transferred with a gas-tight syringe to a sealed vial into which 1 mL of 1 M HCl was added. The acidified cell suspension was shaken vigorously to liberate CO_2, which was quantified by gas chromatography (GC; Hewlett-Packard 5890 Series II) using a Supelco column (80/100 PORAPAK N; 6 feet $\times$ 1/8 inch $\times$ 2.1 mm) coupled to a thermal conductivity detector. Fermentative H_2 production was quantified from 400 μL of head space gas withdrawn from sealed anaerobic vials and analyzed by GC (an Agilent Technologies 7890 GC system) using a Supelco column (60/80 mol sieve 5A; 6 feet $\times$ 1/8 inch) coupled to a thermal conductivity detector.

ADH1 Complementation Construct

The 2,862-bp *Chlamydomonas ADH1* coding sequence was amplified from oligo(dT)-retrotranscribed cDNA using primers *Nde*IADH1Fw (5′-CATATG-ATGTCCTCCAGCCTC-3′, introducing an *Nde*I site at the 5′ end) and ADH1-Rev (5′-GGAGTTCTTCTCCAAGATCAACTAA-3′), and the product was cloned into pGEM T-Easy (Promega). A pGEM T-Easy plasmid with the *ADH1* coding sequence oriented SP6 to T7 (5′ to 3′) was digested with *Nde*I and *Eco*RI, which allowed directional cloning into plasmid pJM43Ble; this vector encodes the protein that confers resistance to the antibiotic Zeocin (Invitrogen) and allows constitutive expression of the cloned cassette under the control of the *PSAD* promoter. Nuclear transformation of the *Chlamydomonas adh1* mutant (*D66* background) was performed with 1.5 μg of pJM43Ble-ADH1 (linearized with *Kpn*I) DNA by the glass bead method (Kindle, 1990). Western-blot analysis was used to screen for *adh1* rescued strains (strains synthesizing the ADH1 protein). The rescued strain was backcrossed two times to *CC-124* and *D66*, and both the mutant and rescued strains were assayed for ethanol accumulation.

Supplemental Data

The following materials are available in the online version of this article.

Supplemental Figure S1. Multiple protein sequence alignment of *C. reinhardtii* ADH1 with homologs from various sources.

Supplemental Figure S2. Protein sequence alignment of *C. reinhardtii* PAT and ACK isoforms.

Supplemental Table S1. List of primers used in the PCR-based mutant screening and in RT-qPCR.

Supplemental Table S2. Intracellular metabolite levels in wild-type and *adh1* cells.

Received November 29, 2011; accepted January 21, 2012; published January 23, 2012.

LITERATURE CITED

Atteia A, van Lis R, Gelius-Dietrich G, Adrait A, Garin J, Joyard J, Rolland N, Martin W (2006) Pyruvate formate-lyase and a novel route of eukaryotic ATP synthesis in Chlamydomonas mitochondria. J Biol Chem **281:** 9909–9918

Atteia A, van Lis R, Mendoza-Hernández G, Henze K, Martin W, Riveros-Rosas H, González-Halphen D (2003) Bifunctional aldehyde/alcohol dehydrogenase (ADHE) in chlorophyte algal mitochondria. Plant Mol Biol **53:** 175–188

Belmans D, van Laere A (1987) Glycerol cycle enzymes and intermediates during adaptation of *Dunaliella tertiolecta* cells to hyperosmotic stress. Plant Cell Environ **10:** 185–190

Catalanotti C, Dubini A, Subramanian V, Yang W, Magneschi L, Mus F, Seibert M, Posewitz MC, Grossman AR (2012) Altered metabolite flow in *Chlamydomonas reinhardtii* mutants lacking pyruvate formate lyase and both pyruvate formate lyase and alcohol dehydrogenase. Plant Cell (in press)

Chen C, Gibbs M (1991) Glucose respiration in the intact chloroplast of *Chlamydomonas reinhardtii*. Plant Physiol **95:** 82–87

Clark DP (1989) The fermentation pathways of *Escherichia coli*. FEMS Microbiol Rev **5:** 223–234

Clark DP, Cronan JE Jr (1980) Escherichia coli mutants with altered control of alcohol dehydrogenase and nitrate reductase. J Bacteriol **141:** 177–183

Cunningham PR, Clark DP (1986) The use of suicide substrates to select mutants of *Escherichia coli* lacking enzymes of alcohol fermentation. Mol Gen Genet **205:** 487–493

Dolferus R, Marbaix G, Jacobs M (1985) Alcohol dehydrogenase in Arabidopsis: analysis of the induction phenomenon in plants and tissue cultures. Mol Gen Genet **199:** 256–264

Dubini A, Mus F, Seibert M, Grossman AR, Posewitz MC (2009) Flexibility in anaerobic metabolism as revealed in a mutant of *Chlamydomonas reinhardtii* lacking hydrogenase activity. J Biol Chem **284:** 7201–7213

Fischer N, Rochaix JD (2001) The flanking regions of *PsaD* drive efficient gene expression in the nucleus of the green alga *Chlamydomonas reinhardtii*. Mol Genet Genomics **265:** 888–894

Gfeller RP, Gibbs M (1984) Fermentative metabolism of *Chlamydomonas reinhardtii*. I. Analysis of fermentative products from starch in dark and light. Plant Physiol **75:** 212–218

Ghirardi ML, Posewitz MC, Maness PC, Dubini A, Yu J, Seibert M (2007) Hydrogenases and hydrogen photoproduction in oxygenic photosynthetic organisms. Annu Rev Plant Biol **58:** 71–91

Ghirardi ML, Togasaki RK, Seibert M (1997) Oxygen sensitivity of algal H_2-production. Appl Biochem Biotechnol **63-65:** 141–151

Ghoshroy S, Binder M, Tartar A, Robertson DL (2010) Molecular evolution of glutamine synthetase II: phylogenetic evidence of a non-endosymbiotic gene transfer event early in plant evolution. BMC Evol Biol **10:** 198–209

Gonzalez-Ballester D, Pootakham W, Mus F, Yang W, Catalanotti C, Magneschi L, Higuera JH, de Montaigu A, Prior M, Galván A, et al (2011) Reverse genetics in Chlamydomonas: a platform for isolating insertional mutants. Plant Methods **7:** 24

Grossman AR, Catalanotti C, Yang W, Dubini A, Magneschi L, Subramanian V, Posewitz MC, Seibert M (2011) Multiple facets of anoxic metabolism and hydrogen production in the unicellular green alga *Chlamydomonas reinhardtii*. New Phytol **190:** 279–288

Gupta KJ, Zabalza A, van Dongen JT (2009) Regulation of respiration when the oxygen availability changes. Physiol Plant **137:** 383–391

Gupta S, Clark DP (1989) *Escherichia coli* derivatives lacking both alcohol dehydrogenase and phosphotransacetylase grow anaerobically by lactate fermentation. J Bacteriol **171:** 3650–3655

Harden A (1901) The chemical action of *Bacillus coli communis* and similar organisms on carbohydrate and allied compounds. J Chem Soc **79:** 610–627

Hemschemeier A, Jacobs J, Happe T (2008) Biochemical and physiological characterization of the pyruvate formate-lyase Pfl1 of *Chlamydomonas reinhardtii*, a typically bacterial enzyme in a eukaryotic alga. Eukaryot Cell **7:** 518–526

Jacobs M, Dolferus R, Van den Bossche D (1988) Isolation and biochemical analysis of ethyl methanesulfonate-induced alcohol dehydrogen-

ase null mutants of *Arabidopsis thaliana* (L.) Heynh. Biochem Genet **26:** 105–122

Kindle KL (1990) High-frequency nuclear transformation of *Chlamydomonas reinhardtii*. Proc Natl Acad Sci USA **87:** 1228–1232

Klein U (1986) Compartmentation of glycolysis and of the oxidative pentosephosphate pathway in *Chlamydomonas reinhardtii*. Planta **167:** 81–86

Klöck G, Kreuzberg K (1989) Kinetic properties of a *sn*-glycerol-3-phosphate dehydrogenase purified from the unicellular alga *Chlamydomonas reinhardtii*. Biochim Biophys Acta **991:** 347–352

Knappe J, Neugebauer FA, Blaschkowski HP, Gänzler M (1984) Post-translational activation introduces a free radical into pyruvate formate-lyase. Proc Natl Acad Sci USA **81:** 1332–1335

Kosourov S, Seibert M, Ghirardi ML (2003) Effects of extracellular pH on the metabolic pathways in sulfur-deprived, H_2-producing *Chlamydomonas reinhardtii* cultures. Plant Cell Physiol **44:** 146–155

Kreuzberg K (1984) Starch fermentation via formate producing pathway in *Chlamydomonas reinhardtii*, *Chlorogonium elongatum* and *Chlorella fusca*. Physiol Plant **61:** 87–94

Kürsteiner O, Dupuis I, Kuhlemeier C (2003) The pyruvate decarboxylase1 gene of Arabidopsis is required during anoxia but not other environmental stresses. Plant Physiol **132:** 968–978

Leonardo MR, Dailly Y, Clark DP (1996) Role of NAD in regulating the *adhE* gene of *Escherichia coli*. J Bacteriol **178:** 6013–6018

Magneschi L, Perata P (2009) Rice germination and seedling growth in the absence of oxygen. Ann Bot (Lond) **103:** 181–196

Mücke U, König S, Hübner G (1995) Purification and characterization of pyruvate decarboxylase from pea seeds (*Pisum sativum* cv. Miko). Biol Chem **376:** 111–117

Mus F, Dubini A, Seibert M, Posewitz MC, Grossman AR (2007) Anaerobic acclimation in *Chlamydomonas reinhardtii*: anoxic gene expression, hydrogenase induction, and metabolic pathways. J Biol Chem **282:** 25475–25486

Ohta S, Miyamoto K, Miura Y (1987) Hydrogen evolution as a consumption mode of reducing equivalents in green algal fermentation. Plant Physiol **83:** 1022–1026

Perata P, Alpi A (1991) Ethanol-induced injuries to carrot cells : the role of acetaldehyde. Plant Physiol **95:** 748–752

Perata P, Vernieri P, Armellini D, Bugnoli M, Tognoni F, Alpi A (1992) Immunological detection of acetaldehyde-protein adducts in ethanol-treated carrot cells. Plant Physiol **98:** 913–918

Philipps G, Krawietz D, Hemschemeier A, Happe T (2011) A pyruvate formate lyase-deficient *Chlamydomonas reinhardtii* strain provides evidence for a link between fermentation and hydrogen production in green algae. Plant J **66:** 330–340

Plaga W, Frank R, Knappe J (1988) Catalytic-site mapping of pyruvate formate lyase: hypophosphite reaction on the acetyl-enzyme intermediate affords carbon-phosphorus bond synthesis (1-hydroxyethylphosphonate). Eur J Biochem **178:** 445–450

Pollock SV, Colombo SL, Prout DL Jr, Godfrey AC, Moroney JV (2003) Rubisco activase is required for optimal photosynthesis in the green alga *Chlamydomonas reinhardtii* in a low-CO_2 atmosphere. Plant Physiol **133:** 1854–1861

Pootakham W, Gonzalez-Ballester D, Grossman AR (2010) Identification and regulation of plasma membrane sulfate transporters in Chlamydomonas. Plant Physiol **153:** 1653–1668

Posewitz MC, King PW, Smolinski SL, Zhang LP, Seibert M, Ghirardi ML (2004) Discovery of two novel radical S-adenosylmethionine proteins required for the assembly of an active [Fe] hydrogenase. J Biol Chem **279:** 25711–25720

Preiss S, Schrader S, Johanningmeier U (2001) Rapid, ATP-dependent degradation of a truncated D1 protein in the chloroplast. Eur J Biochem **268:** 4562–4569

Sadka A, Lers A, Zamir A, Avron M (1989) A critical examination of the role of *de novo* protein synthesis in the osmotic adaptation of the halotolerant alga Dunaliella. FEBS Lett **144:** 93–98

Saika H, Matsumura H, Takano T, Tsutsumi N, Nakazono M (2006) A point mutation of *Adh1* gene is involved in the repression of coleoptile elongation under submergence in rice. Breed Sci **56:** 69–74

Sambrook J, Fritsch EF, Maniatis T (1989) Molecular Cloning: A Laboratory Manual. Cold Spring Harbor Laboratory Press, Cold Spring Harbor, NY

Schnell RA, Lefebvre PA (1993) Isolation of the Chlamydomonas regulatory gene *NIT2* by transposon tagging. Genetics **134:** 737–747

Sizova I, Fuhrmann M, Hegemann P (2001) A *Streptomyces rimosus aphVIII* gene coding for a new type phosphotransferase provides stable antibiotic resistance to *Chlamydomonas reinhardtii*. Gene **277:** 221–229

Steunou AS, Bhaya D, Bateson MM, Melendrez MC, Ward DM, Brecht E, Peters JW, Kühl M, Grossman AR (2006) *In situ* analysis of nitrogen fixation and metabolic switching in unicellular thermophilic cyanobacteria inhabiting hot spring microbial mats. Proc Natl Acad Sci USA **103:** 2398–2403

Tarmy EM, Kaplan NO (1968) Kinetics of *Escherichia coli* B D-lactate dehydrogenase and evidence for pyruvate-controlled change in conformation. J Biol Chem **243:** 2587–2596

Terashima M, Specht M, Naumann B, Hippler M (2010) Characterizing the anaerobic response of *Chlamydomonas reinhardtii* by quantitative proteomics. Mol Cell Proteomics **9:** 1514–1532

Tsygankov AA, Kosourov S, Seibert M, Ghirardi ML (2002) Hydrogen photoproduction under continuous illumination by sulfur-deprived, synchronous *Chlamydomonas reinhardtii* cultures. Int J Hydrogen Energy **27:** 1239–1244

Whitney LA, Loreti E, Alpi A, Perata P (2011) Alcohol dehydrogenase and hydrogenase transcript fluctuations during a day-night cycle in *Chlamydomonas reinhardtii*: the role of anoxia. New Phytol **190:** 488–498

Zabalza A, van Dongen JT, Froehlich A, Oliver SN, Faix B, Gupta KJ, Schmälzlin E, Igal M, Orcaray L, Royuela M, et al (2009) Regulation of respiration and fermentation to control the plant internal oxygen concentration. Plant Physiol **149:** 1087–1098

Zhu J, Shimizu K (2005) Effect of a single-gene knockout on the metabolic regulation in *Escherichia coli* for D-lactate production under microaerobic condition. Metab Eng **7:** 104–115